РАДИОФИЗИКА ТВЕРДОГО ТЕЛА И ПЛАЗМЫ

УДК 539.2.029.64:539.9

STOP BANDS IN MAGNETO-PHOTONIC CRYSTAL IN MILLIMETER WAVEBAND

M. K. Khodzitsky

A. Usikov Institute of Radiophysics and Electronics of the national Academy of Science of Ukraine
12, Ac. Proscury St., 61085, Kharkov, Ukraine
E-mail: khodzitskiy@yandex.ru

One-dimensional (*1D*) magneto-photonic crystal (*MPC*) with tri-layer cell (vacuum-ferrite-quartz) interfaced with wire medium (*WM*) was investigated at microwave band. The appearance of two stopbands associated correspondingly with wave interference in the *MPC* and with ferromagnetic resonance absorption in ferrite layer was demonstrated. The occurrence of surface waves for the *MPC*+*WM* system in the *MPC* stop band frequency range was shown theoretically and experimentally. The surface wave peak allows the tuning of its position with applied magnetic field. It was shown that the steepness of the curve describing the dependence of surface wave peak position on magnetic field is less than the steepness of the corresponding curve for the left edge of the *MPC* stop band. The considered effects will make it possible to develop new magneto tunable microwave devices on basis of magneto-photonic crystals for GHz and THz band. Figs. 5. Ref.: 27 titles.

Key words: magneto-photonic crystal, wire medium, stop band, surface wave, Tamm state, ferromagnetic resonance.

During the last decade, structures with periodic refraction index (known also as photonic crystals (*PC*s) or photonic band gap materials [1]) have been a subject of experimental and theoretical research due to their prominent spectral properties and possibilities of promising applications in microwave and optoelectronics [2–6]. The *PC*s possess band gaps in which electromagnetic wave propagation is prohibited in any direction. Characteristics of band gap can be described by energy band structure or stop band (forbidden band) in transmission spectrum. Substantially, *PC*s are artificially made from dielectric (organic) or metallic materials for band gap electronic control [7–8]. Up to the present, magnetic materials for *PC*s have not attracted much attention because permeability of magnetic materials in the optical frequency range equals to unity. But for ferrites, yttrium iron garnets, granular magnetic films and other magnetic materials the permeability differs from unity at microwave frequencies because of ferromagnetic resonance (*FMR*) [9]. So, ferrites can be exploited for microwave magnetic photonic crystals (*MPC*s) [10]. The ferrites in saturation state have a tensor permeability tuned by a static magnetic field. Therefore, magnetic materials included in *MPC*s make it possible to design the magneto-tunable microwave devices on basis of *MPC*s [11]. Recently, some papers have been devoted to the *MPC*s investigation. Sigalas et al. [12] have studied theoretically the effect of permeability on the photonic band gaps of *MPC*s. A. Saib et al. [13] have studied experimentally magnetic photonic band-gap material based on ferromagnetic nanowires at microwaves. S. Chernovtsev et al. [14, 15] have experimentally and theoretically studied the tuning of frequency stop bands for *1D MPC* on basis of ferrite in *K* and *Ka* frequency band. Jie Xu et al. [16] have experimentally and theoretically investigated the transmission characteristics of *2D MPC* in *X* frequency band. However, in all these works, it has not considered the possibility of appearance of two stopbands: the stop band associated with wave interference in *MPC* (further let's call it as *MPC* stopband) and the stop band associated with resonance absorption in magnetic layer connected with *FMR* (further let's call it as *FMR* zone).

The origin of the usual *PC* stop bands is the same as in the solid state periodical lattice, where the diffraction of electron wave on periodical potential make it impossible for electron with certain energy to move through the crystal. If we proceed with this analogy further we can anticipate the existence of some surface waves (*SW*), (analogous to so named «Tamm states» (*TS*) in solid state physics) [17] on the interface between the *PC* and the medium, where electromagnetic wave cannot propagate (ideally conducting metals, medium with negative permittivity and permeability, another *PC* or *MPC*). The frequency of such surface wave should lie in a forbidden gap of *PC*. The electromagnetic wave vector is directed along the crystal axis, the field being uniform in transversal direction and do not transfer energy. The surface wave can be detected by studying transmission and reflection spectra of the system – a narrow peak appears in the transmission spectrum together with a dip in the reflection spectrum. These surface waves have been theoretically and experimentally studied by Vinogradov et all. for *PC* as well as *MPC* with bi-layered cell in optical frequency range [18–19]. The research of these waves in the microwave band has a very short history is started only recently [20, 21].

In this paper we have experimentally studied appearance of two stopbands with various physical origins in the *MPC* transmission spectrum and occur-

rence of the surface waves in these stopbands in microwave band (22–40 GHz). This frequency band displays certain advantage over the optical band because we can experimentally observe the field distribution near the *PC* interface. Experimental results are in good agreement with theoretical results.

1. Theory. Let us consider the finite structure consisting of *MPC* and *WM*, loaded in a rectangular waveguide (Fig. 1).

1*D MPC* consisted of tri-layer primitive cells (vacuum-ferrite-quartz). The *MPC*s is restricted by a rectangular waveguide along the *y* and *x* axes. A static magnetic field is applied along the *y* axis.

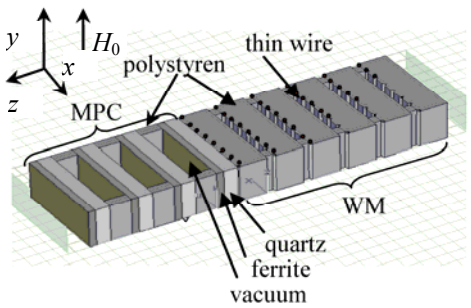

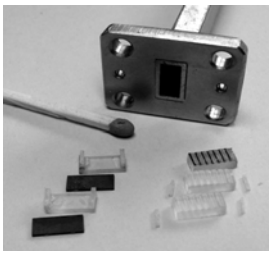

Fig. 1. Schema of structure consisting of the MPC and WM, loaded in a rectangular waveguide

It is well known that the ferrite layers, magnetized under the external magnetic field have a tensor permeability derived from the Landau-Lifshitz equations [22]:

$$\ddot{\mu} = \begin{bmatrix} \mu & j\mu_a & 0 \\ -j\mu_a & \mu & 0 \\ 0 & 0 & 1 \end{bmatrix}. \qquad (1)$$

For saturated ferrite with dissipation we have

$$\mu = \frac{\omega_H(\omega_H + \omega_M) - \omega^2}{\omega_H^2 - \omega^2}; \qquad (2)$$

$$\mu_a = \frac{\omega_M \omega}{\omega_H^2 - \omega^2}, \qquad (3)$$

where $\omega_H = \gamma H_0 + j\alpha\omega$ is the ferromagnetic resonance frequency; γ is the gyromagnetic ratio; H_0 is the dc magnetic field in ferrite layers; $\omega = 2\pi f$ is the circular frequency of the alternating electromagnetic field; α is the damping coefficient of ferrites; $\omega_M = \gamma 4\pi M_S$ is the characteristic frequency of ferrite; M_S is the ferrite saturation magnetization.

Let us consider the propagation of a plane wave through ferrite. The wave vector is normal to the applied static magnetic field H_0 (this case is called transverse magnetization), the tensor of effective permeability can reduce to a scalar as [22]:

$$\mu_{eff} = \frac{\mu^2 - \mu_a^2}{\mu}. \qquad (4)$$

The midgap frequencies of usual *MPC* stop bands are defined as [23]:

$$f_C = \frac{c}{m\lambda_C};\ m\lambda_C = 2(n_v d_v + n_f d_f + n_q d_q), \qquad (5)$$

where c is the speed of light; m is the number of *MPC* stop band; d_v, d_f, d_q are thicknesses of vacuum, ferrite and quartz layers correspondingly; n_v, n_f, n_q are refraction indexes of vacuum, ferrite and quartz layers correspondingly which are evaluated as

$$n_v = 1;\ n_f = \sqrt{\varepsilon_f \mu_{eff}};\ n_q = \sqrt{\varepsilon_q}, \qquad (6)$$

where ε_q, ε_f are the permittivity of quartz and ferrite layers correspondingly.

The *MPC* is adjacent through the quartz layer to *WM*. *WM* represents the arrays of thin copper wires on polystyrene substrate. The metallic wires were structured on a scale much less than the wavelength of radiation. When the wavelength of the incident radiation is much larger than the size and spacing of scatterers, the response of the scatterers to the incident fields can be treated by way of the effective medium theory. Therefore, an effective permittivity ε_{eff} can be used to define the permittivity of the medium. Negative permittivity of *WM* can be achieved at microwave frequencies (permittivity is negative below plasma frequency ω_p). The *WM* effective permittivity and the plasma frequency are given by formula [24]:

$$\varepsilon_{eff} = \varepsilon_{host} - \frac{{\omega_p}^2}{\omega^2};\ {\omega_p}^2 = \frac{2\pi c^2}{a^2 \ln(a/r)}, \qquad (7)$$

where a is the lattice parameter (the distance between the nearest wires); r is the radius of the wires; ε_{host} – host medium.

To obtain the surface wave (analogous to so-called Tamm state) it is necessary that a *MPC* stop band overlaps the frequency range where effective permittivity of *WM* has negative sign.

The well-known transfer matrix technique [15, 23] was used to find the transmission (reflection) coefficient for periodical *MPC* structure (Fig. 1). The finite-difference-time-domain method (*FDTD*) well-described anywhere [25–27] was used to calculate the transmission (reflection) spectra of *WM* and

MPC+WM and to evaluate the field profile of the surface wave as well.

2. Experiment. To carry out the experimental investigations, the *MPC* and the *WM* were designed and fabricated. The ferrite layer (brand *1SCH4*) has complex permittivity of about $\varepsilon_f = 11{,}1 + j0{,}0008$, saturation magnetization of $M_S = 382Gs$, damping coefficient of $\alpha = 0{,}024$ and thickness of $d = (0{,}5 \pm 0{,}02)$ mm. The quartz layer has permittivity of about $\varepsilon_q = 4{,}5$ and thickness of $d = (1 \pm 0{,}02)$ mm. The vacuum layer has thickness of $d = (1{,}5 \pm 0{,}02)$ mm. The *MPC* has 4 tri-layered cells and interfaced with *WM* by quartz layer. According to equations (5), (6) for given parameters the midgap frequency of the first *MPC* stop band associated with wave interference in *MPC* is about of 28,37 GHz at zero applied magnetic field ($\mu_{eff} = 1$). The *WM* consists of polystyrene substrate (thickness of 2,1 mm, permittivity $\varepsilon_{host} = 2{,}53$) with thin copper wires on one side. The gap between the polystyrene substrates is 0,5 mm. The polystyrene substrate has wires with length of 3,3 mm and diameter of 0,15 mm. The distance between two nearest wires is of 1 mm along x axis. The *WM* has 6 polystyrene substrates with 8, 8, 8, 6, 5, 3 wires accordingly. According to equations (7) such *WM* has negative effective permittivity till plasma frequency of 74,36 GHz.

The experimental setup includes mainly the vector network analyzer (*VNA*), waveguide transmission line, waveguide segment with structure under study and electromagnet controlled by power supply unit (the magnetic field range is about of 0–7000 Oe) [14, 15]. The composite structure was loaded in a rectangular waveguide segment with cross-section of 7,2×3,4 mm^2. The segment with structure under study was placed between poles of electromagnet where a uniform static magnetic field was provided. An *EM* wave propagates along the z axis with an electric field along the y axis and magnetic field along the x axis (Fig. 1). The static magnetic field was applied normally to alternating magnetic field. The transmission spectra were automatically measured by the *VNA* in the frequency range of 22–40 GHz.

3. Results and discussions. Let's consider transmission spectra for various structures namely: for *MPC*; for *WM*; for *MPC+WM*.

The transmission spectra of the *MPC* have been measured and calculated using transfer matrix technique [15, 23] and effective permeability has been calculated using the equation (4). The results are shown in Fig. 2, a–c. For small applied magnetic field: $\mathrm{Re}(\mu_{eff}) \in (0,1)$ the transmission spectra of the MPC have a shape of smooth upturned dome and represent stop-band associated with Bragg interference in periodical *MPC* (*MPC* stop band). The bottom value of stop-bands depth (the difference between transmission coefficient in pass-band and one in stop-band) equals approximately to –40 dB. As the magnetic field increases the position of stop band edges shifts weakly to higher frequencies. The simulation corroborates the experimental results, though with some discrepancy, associated with an error in the simulation parameters choice: the module of transmission coefficient is defined by imaginary part of both constitutive parameters ($\dot{\varepsilon}$, $\dot{\mu}$) of each *MPC* layer while the positions of *MPC* stop-band edges are defined by real part of parameters.

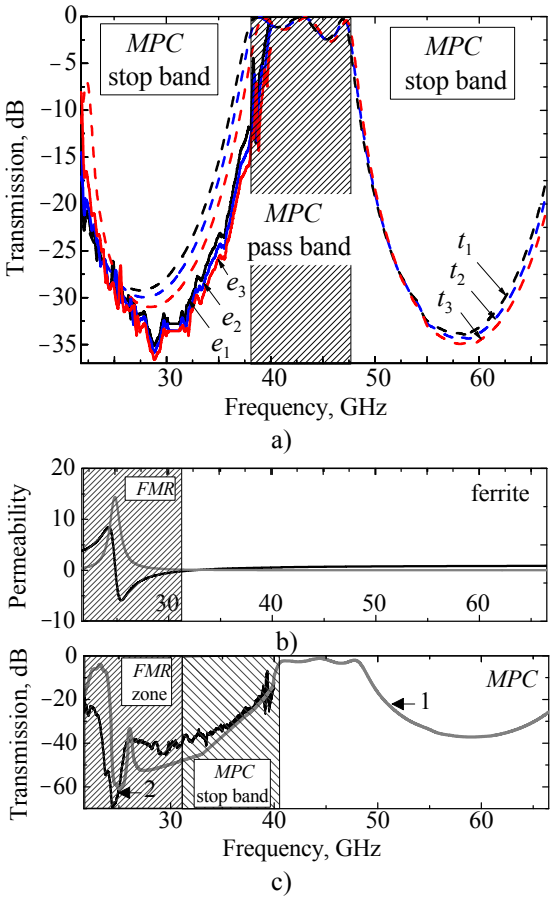

Fig. 2. Transmission spectrum of the *MPC* for various applied magnetic fields at $\mathrm{Re}(\mu_{eff}) \in (0,1)$, theory: t_1 – H = 1130 Oe, t_2 – H = 2290 Oe, t_3 – H = 3370 Oe; experiment: e_1 – H = 1130 Oe, e_2 – H = 2290 Oe, e_3 – H = 3370 Oe (a); frequency dispersion of effective permeability of ferrite at H = 6840 Oe (b); experimental (black line) and simulated (grey line) transmission spectrum of the *MPC* for H=6840 Oe at $\mathrm{Re}(\mu_{eff}) \in (-6,8)$ correspondingly (c)

For large magnetic field (H = 6840 Oe) the permeability becomes negative $\mathrm{Re}(\mu_{eff}) \in (-6,8)$ in the investigated frequency range. The depth of experimental *MPC* transmission spectrum drops down to –70 dB see Fig. 2, c. The frequency position of the valley coincides with ferromagnetic resonance fre-

quency. We can conclude that a new absorption process connected with *FMR* in ferrite was engaged. Hence we have two deep valleys and correspondingly two stop-bands with various origins. The first band (the *FMR* zone) in the range from 23 to 31 GHz corresponds to the *FMR* absorption (Fig. 2, b). In this frequency range the real part of effective permeability of the ferrite is negative and imaginary part is different from zero, therefore electromagnetic wave can not propagate in ferrite. The position of mid-gap frequency in this band is defined by ferromagnetic resonance frequency and varies linearly with the static magnetic field. The second band (*MPC* stop band) in the range from 31 to 41 GHz corresponds to known Bragg interference in *MPC*. In this frequency range the electromagnetic power is not absorbed. The position of mid-gap frequency in this band is defined by the equation (5) and remains almost unchanged at variations of the magnetic field. This behavior is due to small variation (from 0 to 1 at 32 GHz) of the effective magnetic permeability throughout the whole interval of static magnetic field change (0–7000 Oe).

Next we consider the transmission spectra for the *WM* (experimental (solid line) and simulated (dash line)) (Fig. 3, a).

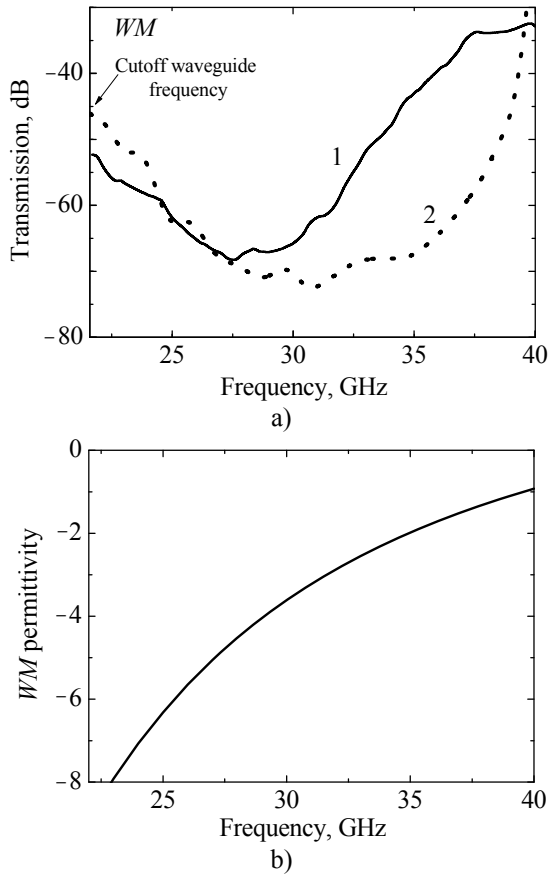

Fig. 3. Transmission spectrum of the wire medium: 1 – experiment; 2 – simulation (a); frequency dispersion of effective wire medium permittivity for following parameters: $a = 1$ mm; $r = 0{,}075$ mm; $\varepsilon_{host} = 2{,}53$ (polystyren) (b)

The deep valley with the bottom level of the order of –70 dB shows the frequency band where the electromagnetic wave can not propagate through the *WM*. Naturally this is connected with negative effective permittivity of the *WM*. The experimental and theoretical curve coincide well within 21–28 GHz. Within higher frequency range (28–40 GHz) the discrepancy between experimental and simulated transmission spectra is associated with the shortcomings of calculation method and wire spacing inaccuracy in the experiment. The effective permittivity of *WM* is negative in the frequency range under study (21–40 GHz) see in Fig. 3, b.

It was shown in [18] that at interface between *MPC* and medium with negative permittivity surface wave could exist. To study surface wave we use the composite system *MPC*+*WM* in the frequency band where effective permittivity of the *WM* is negative. The surface wave appears as a sharp peak in the transmission (reflection) spectra in the *MPC* stop-band and is detected experimentally (Fig. 4, a).

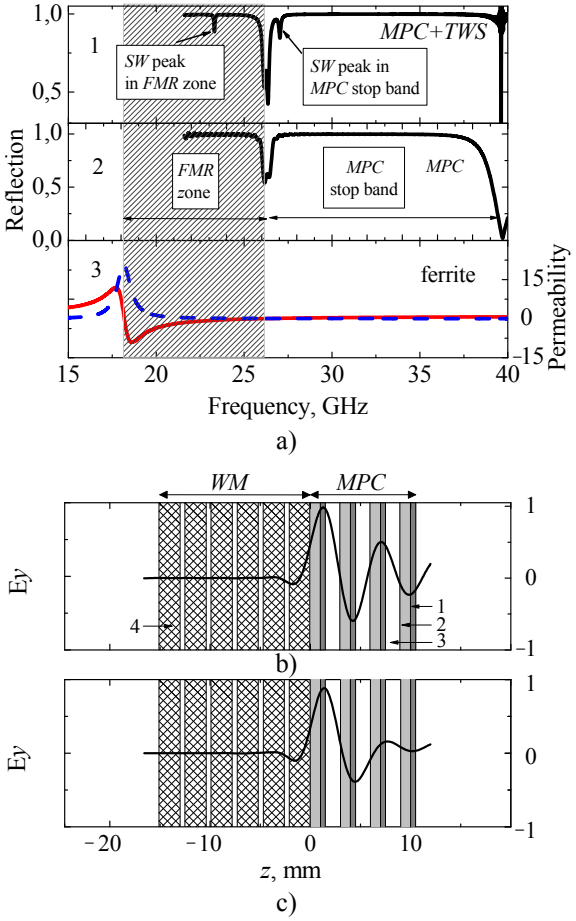

Fig. 4. 1 – Simulation of reflection spectrum of the *MPC*+*WM* at $H = 4560$ Oe, 2 – Simulation of reflection spectrum of the *MPC* at $H = 4560$ Oe, 3 – Frequency dependence of permeability of ferrite at $H = 4560$ Oe (a); Calculated *Ey* field profile along *z* axis of the *SW* peak in *MPC* stopband at $f = 27{,}04$ GHz (b) and *SW* peak in *FMR* zone at $f = 23{,}31$ GHz (c) for *MPC*+*WM* case at $H = 4560$ Oe (1 – ferrite, 2 – quartz, 3 – vaccum, 4 – polystyrene with wires)

It worth noting here that we detected one more peak in the *FMR* zone as well. This peak may correspond also to surface wave (*SW*). The calculated *Ey* field profiles along *z* axis of both surface waves are shown in Fig. 4, b, c at $H = 4560$ Oe. The reflection spectrum of the *MPC+WM* structure with surface waves in the *MPC* and *FMR* stop bands at magnetic field of 4560 Oe are shown in the Fig. 4, a. To study the «three layer» *MPC* it is necessary to derive the corresponding dispersion equation for this periodical structure and calculate the frequency position of the surface wave peak. As can be seen from the Fig. 4, a the little quasi-pass band occurs between the *MPC* and *FMR* stop band. Indeed it's the strongly changed at the left edge of *MPC* band due to close neighborhood to the *FMR* absorption band.

To demonstrate the possibility of magnetic field to tune of *SW* peak position, the corresponding experiment and calculation were carried out. The experimental and simulated evolution of the *SW* peak position in the *MPC* stop band with variation of the magnetic field are shown in the Fig. 5.

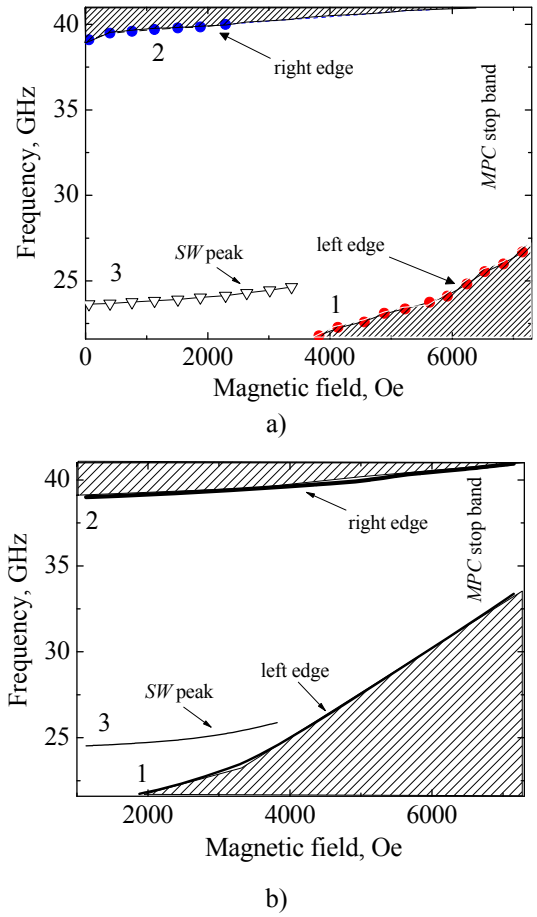

Fig. 5. Experimental frequency dependence of MPC stop band edges (1, 2) and surface wave peak (3) position on applied magnetic field (a); calculated frequency dependence of MPC stop band edges (1, 2) and surface wave peak (3) position on the magnetic field (b)

Experimental results are in good agreement with the results of simulation. The tuning of *SW* peak position is about 1 GHz on 3 kOe. It should be noted, the calculated frequency dependence of surface wave peak position on magnetic field is shown in the Fig. 5, b only for corresponding experimental data. It should be noted that the steepness of the curve describing the dependence of the *SW* peak position in change on magnetic field ($\partial f_{SW}/\partial H_{\exp} = 0{,}42$ GHz/kOe, $\partial f_{SW}/\partial H_{theory} = 0{,}7$ GHz/kOe) is less than the corresponding steepness of the left edge of the *MPC* stop band ($\partial f_{Leftedge}/\partial H_{theory} = 1{,}39$ GHz/kOe). The range of magnetic field is 1880–3370 Oe. Such behavior can be explained by the strong dependence of *SW* peak position on the impedance of bounding medium which is not sensitive in the case of wire media without magnetic inclusions to the applied magnetic field.

Conclusions. The transmission and reflection spectra of one-dimensional *MPC* with tri-layer cell interfaced with *WM* were investigated at microwave band.

The appearance of two stopbands: stopband connected with wave interference in *MPC* and one connected with ferromagnetic resonance absorption in ferrite layer was demonstrated.

For *MPC+WM* structure it is shown experimentally and theoretically the occurrence of surface waves (analogous to «Tamm states») in the frequency range corresponding to the *MPC* stop band.

The tuning of the surface wave peak position by magnetic field was demonstrated. The steepness of the curve describing the dependence of the surface wave peak position on the magnetic field is less than the corresponding steepness of the left edge of *MPC* stop band.

The studied effects make it possible to design the new magnetotunable devices on basis of *MPC*s for GHz and THz bands.

I acknowledge helpful discussions with Prof. S. I. Tarapov and D. P. Belozorov. This work was supported by the *STCU* Project No. 4912 and the Grant of the President of Ukraine for young scientists.

1. *Yablonovitch E.* Inhibited Spontaneous Emission in Solid-State Physics and Electronics // Phys. Rev. Lett. – 1987. – 58, No. 20. – P. 2059–2062.
2. *Radistic V., Qian Y. X., Coccioli R. et al.* Novel 2-*D* photonic bandgap structure for microstrip lines // IEEE Microwave Guided Wave Lett. – 1998. – 8, No. 1. – P. 69–71.
3. *Yun T. Y., Chang K.* Uniplanar one-dimensional photonic-bandgap structures and resonators // IEEE Trans Microwave Theory and Techniques. – 2001. – 49, No. 3. – P. 549–553.
4. *Th'evenot M., Reineix A.* Directive photonic-bandgap antennas // IEEE Trans Microwave Theory and Techniques. – 1999. – 47, No. 11. – P. 2115–2122.

5. *Colburn J. S., Rahmat-Samii Y.* Patch antennas on externally perforated high dielectric constant substrates // IEEE Trans. Antennas Propagat. – 1999. – 47, No. 12. – P. 1785–1794.
6. *Lourtioz J.-M., de Lustrac A.* Metallic photonic crystals // C. R. Phys. – 2002. – 3, No. 1. – P. 79–88.
7. *Yun Tae-Yeoul, Chang Kai*. An electronically tunable photonic bandgap resonator controlled bypiezoelectric transducer // Proc. of IEEE MTT-S International Microwave Symposium. – 2000. – 3. – P. 1445–1447.
8. *Chen Hou-Tong, Hong Lu, Azad A., Averitt R. et al.* Electronic control of extraordinary terahertz transmission through subwavelength metal hole arrays // Optics Express. – 2008. – 16**,** No. 11. – P. 7641–7648.
9. *Kittel C.* Introduction to Solid State Physics. – N. Y.: Wiley & Sons, 1994. – 646 p.
10. *Lyubchanskii I. L. et al.* Magnetic photonic crystals // J. Phys. D: Appl. Phys. – 2003. – 36**,** No. 18. – P. R277–R287.
11. *Kee C., Park I., Lim H. et al.* Microwave photonic crystal multiplexer and its applications // Curr. Appl. Phys. – 2001. – 1, No. 1. – P. 84–87.
12. *Sigalas M. M., Soukoulis C. M., Biswas R. et al.* The effect of the magnetic permeability on photonic band gaps // Phys. Rev. B. – 1997. – 56, No. 3. – P. 959–962.
13. *Saib A., Vanhoenacker-Janvier D., Huynen I.* Magnetic photonic band-gap material at microwave frequencies based on ferromagnetic nanowires // Appl. Phys. Letters. – 2003. – 83, No. 12. – P. 2378–2380.
14. *Chernovtsev S. V., Pavlov A. I., Tarapov S. I.* Simulation of magnetically controllable photonic bandgap structures // Proc. of SPIE Photonic North. – 2007. – P. 67961A–1–67961A-11.
15. *Chernovtsev S. V., Tarapov S. I., Belozorov D. P.* Magnetically controllable 1D magnetophotonic crystal in millimeter wavelength band // J. Phys. D: Appl. Phys. – 2007. – 40, No. 2. – P. 295–299.
16. *Jie Xu, Rui-xin Wu, Ping Chen, Yue Shi.* Transmission characteristics of two-dimensional magnetized magnetic photonic crystals // J. Phys. D: Appl. Phys. – 2007. – 40, No. 4. – P. 960–963.
17. *Tamm I. Y.* On a Possible Manner of Electron Binding to Crystal Surfaces // Phys. Z. Sowjetunion. – 1932. – 1. – P. 733–746.
18. *Vinogradov A. P., Dorofeenko A. V., Erokhin S. G. et al.* Surface state peculiarities in one-dimensional photonic crystal interfaces // Phys. Review B. – 2006. – 74, No. 4. – P. 045128–045136.
19. *Merzlikin A. M., Vinogradov A. P., Dorofeenko A. V. et al.* Controllable Tamm states in magnetophotonic crystal // Physica B: Condensed Matter. – 2007. – 394, No. 2. – P. 277–280.
20. *Khodzitskiy M. K.* Spatial field localization in mirror – reflected magnetophotonic crystal with tri-layer cell // Proc. of Int. conf. Days of Diffraction. – 2008. – P. 83.
21. *Khodzitskiy M. K., Tarapov S. I.* Spectra for 1D magnetophotonic crystal with tri-layer cell interfaced with metallic structures at microwave band // Proc. of 12th Int. conf. MMET. – 2008. – P. 524–526.
22. *Gurevich A.G., Melkov G.A.* Magnetization Oscillations and waves. – New York: CRC Press, 1996. – 445 p.
23. *Born M., Wolf E.* Principles of Optics. – Cambridge: University Press, 2002. – 986 p.
24. *Pendry J. B., Holden A. J., Robbins D. J., Stewart W. J.* Low frequency plasmons in thin-wire structures // J. Phys.: Condensed Matter. – 1998. – 10, No. 22. – P. 4785–4809.
25. *Miller E. K.* Time-Domain modeling in electromagnetics // IEEE J. of El. Waves and Applications. – 1994. – 8, No. 9/10. – P. 1125–1172.
26. *Taflove A.* Computational Electrodynamics: The Finite-Difference Time-Domain Method. – Boston: Artech House, 1995. – 599 p.
27. *Miller E. K., Poggio A. J., Burke G. J.* An Integro-Differential Equation Technique for the Time-Domain Analysis of Thin Wire Structures // Journ. of Computational Physics. – 1973. – 12. – P. 24–48.

ЗОНЫ НЕПРОПУСКАНИЯ В МАГНИТОФОТОННОМ КРИСТАЛЛЕ В МИЛЛИМЕТРОВОМ ДИАПАЗОНЕ ДЛИН ВОЛН

М. К. Ходзицкий

Был исследован одномерный магнитофотонный кристалл (МФК) с трехслойной ячейкой (воздух-феррит-кварц), ограниченный проволочной средой в миллиметровом диапазоне длин волн. Показано появление двух зон непропускания, связанных соответственно с интерференцией волн в МФК и с ферромагнитно-резонансным поглощением в ферритовом слое. Показано теоретически и экспериментально появление поверхностных волн для системы МФК+проволочная среда в частотном диапазоне зоны непропускания МФК. Показана возможность управления положением пика пропускания, связанного с поверхностной волной в спектре с помощью магнитного поля. Показано, что крутизна кривой, описывающая зависимость положения пика пропускания, связанного с поверхностной волной от магнитного поля, меньше, чем крутизна кривой, описывающая зависимость положения низкочастотного края зоны непропускания МФК от магнитного поля. Рассматриваемые эффекты позволят разработать новые магнитоуправляемые микроволновые устройства на основе МФК в гигагерцевом и терагерцевом диапазонах.

Ключевые слова: магнитофотонный кристалл, проволочная среда, зона непропускания, поверхностная волна, Таммовское состояние, ферромагнитный резонанс.

ЗОНИ НЕПРОПУСКАННЯ В МАГНІТОФОТОННОМУ КРИСТАЛІ В МІЛІМЕТРОВОМУ ДІАПАЗОНІ ДОВЖИН ХВИЛЬ

М. К. Ходзицький

Було досліджено одновимірний магнітофотонний кристал (МФК) із тришаровою коміркою (воздух-ферит-кварц) обмежений дротовим середовищем у міліметровому діапазоні довжин хвиль. Показано появу двох зон непропускання зв'язаних відповідно з інтерференцією хвиль у МФК і з ферромагнітно-резонансним поглинанням у ферритовом шарі. Показано теоретично й експериментально появу поверхневих хвиль для системи МФК+дротове середовище у частотному діапазоні зони непропускання МФК. Показано можливість керування положенням піка пропускання пов'язаного з поверхневою хвилею в спектрі за допомогою магнітного поля. Показано, що крутизна кривої, що описує залежність положення піка пропускання, пов'язаного с поверхневою хвилею від магнітного поля, менше, ніж крутизна кривої, що описує залежність положення низькочастотного краю зони непропущення МФК від магнітного поля. Розглянуті ефекти дозволять розробити нові магнітокеровані мікрохвильові пристрої на основі МФК у гигагерцевому і терагерцевому діапазонах.

Ключові слова: магнітофотонный кристал, дротове середовище, зона непропускання, поверхнева хвиля, Таммовський стан, феромагнітний резонанс.

Рукопись поступила 7 мая 2009 г.